

ANTICANCER EFFECT OF AgTOEPyP4 PORPHYRIN

N. H. KARAPETYAN ^{1*}, G. V. ANANYAN ^{2**}, S. G. HAROUTIUNIAN ^{1,3***}¹ *Laboratory of Physics of Macromolecules, Research Institute of Physics, YSU, Armenia*² *Interfaculty Scientific-Research Laboratory of Structural Biophysics, YSU, Armenia*³ *Joint Institute for Nuclear Research, Dubna, Russian Federation*

The silver-containing porphyrin Ag-*meso*-tetra(4-N-hydroxyethylpyridyl) porphyrin (AgTOEPyP4) was investigated as a potential anticancer drug using spectrophotometric, calorimetric and electrophoretic measurements. The studies were conducted on healthy, cancer-induced, and treated by AgTOEPyP4 white mice. DNA was isolated from the liver and tumor tissues of mice. Melting curves were studied in the presence of various stoichiometric concentrations of Mn²⁺ ions. The character of the DNA–Mn²⁺ interaction in the tumor differs from that in the norm due to defects in the secondary structure of tumor DNA, which is expressed in the DNA melting characteristics of DNA. It was revealed that the melting parameters, enthalpy, and electrophoretic mobility of DNA isolated from the tumor-bearing mice tissues differed from healthy DNA. It was shown that all studied parameters of the DNA isolated from the liver and tumor treated by AgTOEPyP4 mice approached the norm. The obtained results revealed that AgTOEPyP4 porphyrin has a pronounced therapeutic effect against sarcoma S180 and requires further investigation as an anticancer drug.

<https://doi.org/10.46991/PYSU:B/2023.57.1.041>

Keywords: porphyrin, cancer DNA, DNA melting, calorimetry, electrophoresis.

Introduction. New compounds based on porphyrins are actively synthesized and studied along with antitumor drugs currently used in clinics. These compounds must meet certain requirements: have a high selectivity for cancer cells and slight retention by normal tissues; they must have low toxicity and are easily excreted from the body, are stable during storage and administration, and fluoresce. The significant efficacy and low toxicity of porphyrins as natural substances, as well as their inertness when interacting with other anticancer drugs, make photodynamic therapy a perspective for further study and application. Photosensitization of porphyrins and cytotoxic response to photodynamic therapy of tumors can involve apoptosis, necrosis or both [1, 2].

* E-mail: nelkh@ysu.am

** E-mail: angay@ysu.am

*** E-mail: sharout@ysu.am

Porphyrins perform many different functions in living organisms, including participation in plant photosynthesis (chlorophyll), oxygen transport (hemoglobin), and redox reactions (cytochromes) [3].

Using fluorescence microscopy, it was shown that photosensitizers are initially adsorbed on the outer membrane of the cell. Within a few hours, depending on the type of photosensitizer, a greater or less part of it passes through the membrane into the cell and then is adsorbed on the membranes of the organelles. The type of organelle, in which the photosensitizer is localized, is also largely determined by its chemical nature. For some substances, high selectivity has been shown in relation to mitochondria, the outer cell membrane or lysosomes. More hydrophilic photosensitizers, as well as aggregates of photosensitizers, are often captured by the cell by pinocytosis and, thus, are localized in lysosomes. In general, it is correct to talk about the distribution of the sensitizer in various cell membranes [4, 5].

Porphyrins can accumulate selectively in cancer cells and can be used as new drugs. The presence of metal, the functional position of the substituent and the alkyl chain length affect the accumulation of porphyrin and its effectiveness. For example, it was found that a series of gold(III) tetraaryl porphyrins is much more effective than cisplatin in killing human cancer cells, including the drug resistant tumor variants [6]. It was shown that the *meso*-derivative showed higher accumulation in cancer cells than the β -derivative, and porphyrins with less bulky substituents actively accumulate in cancer cells. Therefore, a *meso*-derivative may have a higher anti-tumor effect than a β -derivative [7]. Being DNA-binding molecules porphyrins can find application in biology and medicine as potential antitumor and antiviral therapeutic drugs [8].

In the present work Ag-*meso*-tetra(4-N-hydroxyethylpyridyl)porphyrin (AgTOEPyP4) was used as an anticancer agent against mice Sarcoma S180. A new synthetic water-soluble AgTOEPyP4 porphyrin is planar molecule and carries a positive charge in periphery radicals. The coordination number of Ag is four and, as a result of this, in the composition of metalloporphyrins, it forms four-coordination bonds with the nitrogen atoms of the porphyrin core.

In this investigation we used the original and relatively new method to study the structural changes in tumor DNA, which was developed at the department of Molecular Physics at YSU [9]. This method allows revealing the conformational state of DNA at the influence of Mn^{2+} metal ions on the DNA intramolecular melting. As opposed to the well-known, classical melting method this method allows more clearly evaluating changes and gets a more pronounced effect of structural changes at the molecular level of DNA. According to modern concepts, nucleotides have three types of binding sites for alkali and transition metal ions: nitrogenous bases, phosphate groups and sugars (ribose or deoxyribose). Sugars are weak ligands and are not of interest as a binding site. Phosphate groups are strong ligands, due to the high density of negative charge localized to oxygen atoms. Nitrogenous bases are also strong ligands for transition metal ions [10].

The DNA melting was performed in the presence of different stoichiometric concentrations of Mn^{2+} ions. It is known that DNA samples from tumor cells have defects in the helical structure. The structural changes may influence the character of the DNA- Mn^{2+} ion interactions, which allows one to reliably detect the structural

differences of DNA isolated from normal and tumor cells. So, this method allows for trustworthy evaluate structural changes in DNA molecules.

The calorimetric and electrophoretic measurements were used also to confirm obtained results.

Materials and Methods. All used chemicals and reagents of analytical reagent grade were obtained from “Sigma-Aldrich”. AgTOEPyP4 (Fig. 1) was synthesized at the Department of Pharmacological Chemistry of the Yerevan State Medical University [11].

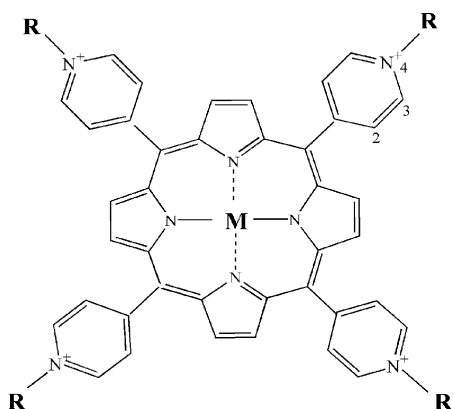


Fig. 1. Chemical structure of Ag-meso-tetra(4-N-hydroxyethylpyridyl)porphyrin.
M=Ag, R=(-CH₂-CH₂-OH).

Experimental Animals. White male outbreed mice of 7 weeks old with a mass of 23±5 g were inoculated with sarcoma S180 (“Sigma”). Sarcoma 180 cells (~10⁶) in 0.1 mL saline were subcutaneously injected into the mice. After 24 h, mice were treated by AgTOEPyP4 porphyrin once a 48 h for 10 days (5 times).

Three groups of animals were taken into consideration:

- I group: healthy animals as control (normal);
- II group: animals inoculated with sarcoma S180;
- III group: mice inoculated with sarcoma S180 and treated by AgTOEPyP4 porphyrin intraperitoneally at the rate of 13 µg/g.

The total dose of five injections was 1.5 mg per mouse. The animals were slaughtered two weeks after the treatment had ended. The tumor was excised and weighed. 7–10 animals for each experimental group were used. This part of experiments carried out in the base of Institute of Fine Organic Chemistry.

During the experiments, all institutional, national and international rules for the use and care of animals were observed.

DNA was isolated by the standard chloroform method as described before [12]. After purification, the optical characteristics of DNA were determined from the ratios $A_{260}/A_{280}=1.8$, $A_{260}/A_{230}=2.0$, which corresponded to the optical characteristics for highly purified DNA [13].

Spectroscopy. The absorption spectra and melting curves of DNA samples were recorded on a Perkin-Elmer Lambda 800 UV/VIS spectrophotometer. All the experiments were carried out in 0.1 SSC buffered saline, 1 SSC content of 0.15 M NaCl and 0.015 M sodium citrate, pH 7.4. DNA concentrations in base pairs were determined spectrophotometrically at $\lambda=260$ nm with $\epsilon = 1.31 \cdot 10^4$ M⁻¹cm⁻¹ [14].

Melting experiments were carried out at 260 nm, with a heating rate of 0.25°C/min, in 25–95°C temperature interval, using 10 mm thermostatic quartz cuvettes. The degree of DNA denaturation $1-\theta$, versus temperature, was calculated using the following formula:

$$1 - \theta = \frac{A - A_{\min}}{A_{\max} - A_{\min}},$$

where θ is the degree of helicity; A , A_{\min} and A_{\max} are the absorbencies of the experimental curve the lower baseline (helix) and the upper baseline (coil), respectively at a given temperature T [15]. The melting temperature (T_m) is defined as the temperature at which half of the total base pairs are “melted”, i.e., $1-\theta = 0.5$ and ΔT the melting interval equaled to the difference of temperatures, at which the tangent in the bend point crosses the levels $\theta=0$ and $\theta=1$, i.e.

$$\Delta T = \left(\frac{\partial \theta}{\partial T} \right)_{T=T_0}^{-1}.$$

The melting of DNA isolated from different mice tissues was investigated in the absence and presence of Mn^{2+} ions, the molar ratios $[Mn^{2+}]/[DNA]$ were in the range of 0–4 M/bp (0 – means the melting without Mn^{2+} ions).

Microcalorimetry. The DNA microcalorimetric curves were obtained on differential adiabatic scanning microcalorimeter DASM-4. The volume of the measuring cell was 0.8 mL, the heating rate was 0.25°C/min, and the temperature range of measurement made was 20–100°C [16]. The values of DNA helix-coil transition enthalpy ΔH was calculated from the area of the melting peak using a Scal Dos program, according to the formula:

$$\Delta H = \int C_p dT,$$

where C_p is a specific heat capacity at the constant pressure. All curves were analyzed with Origin 7.

Agarose Gel Electrophoresis. The DNA samples containing 3 μg DNA were analyzed by electrophoresis in 1% agarose gel using Tris-boric acid–EDTA buffer, pH 8.0, at voltage 5 V/cm. The gel was stained with ethidium bromide (at 0.5 ng/mL) and photographed under UV-transilluminator. The 1 kb DNA Ladder (“Promega Product”, Fitchburg, Wisconsin) was used as a marker for determining the size of DNA from 0.25 to 10 kbp [17].

All presented data were averages of 3–4 studies. The experimental data were statistically processed. For all studied parameters the values of standard deviations were calculated [18].

Results. The anticancer effect of AgTOEPyP4 was carried out by index of tumor suppression (ITS):

$$ITS = \frac{MTW_{\text{tumor}} - MTW_{\text{treated}}}{MTW_{\text{tumor}}} 100\%,$$

where MTW_{tumor} is middle tumor weight; MTW_{treated} is middle tumor weight after treated with AgTOEPyP4 [19]. The value of ITS, calculated for treated by AgTOEPyP4 porphyrin, was 57%.

DNA was isolated from all investigated groups and compared with healthy mice liver DNA. Detection of DNA structural changes is characterized by their melting curves. The changes in melting temperature (T_m) and interval of helix-coil transition (ΔT) indicate damage to the secondary structure of DNA.

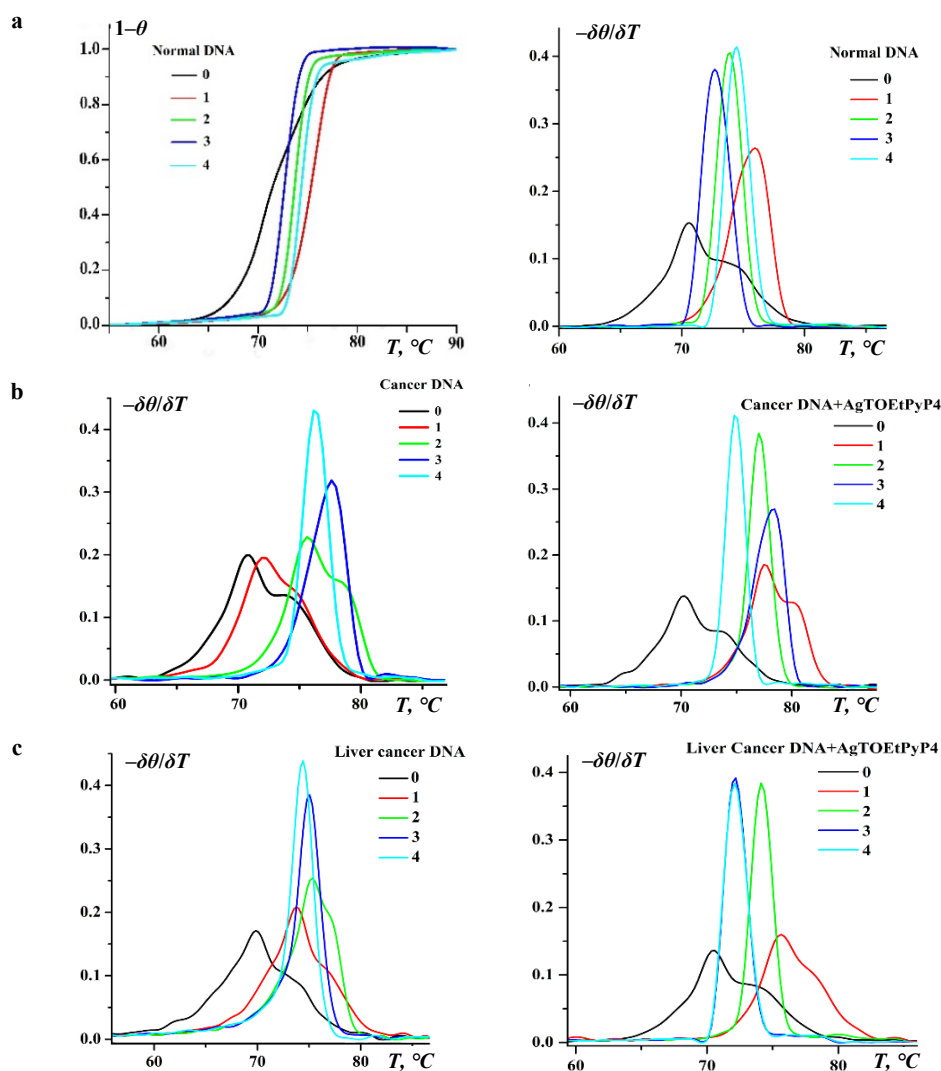


Fig. 2. a) Integral and differential melting curves of DNA isolated from a healthy (normal) mice liver; b) differential melting curves of DNA from untreated and treated with AgTOEPyP4 porphyrin mice tumor tissues; c) differential melting curves of DNA from untreated and treated with AgTOEPyP4 porphyrin mice liver tissues.

DNA melting was carried out in the presence of Mn^{2+} ions at different stoichiometric concentrations (0–4 M Mn^{2+} per one mole nucleotide).

The obtained experimental melting curves were normalized and differenced (see Table and Fig. 2). Differential melting curves reveal the fine structure of DNA melting. The melting parameters of DNA isolated from the tumor-diseased mice tissues differ from healthy DNA. Thus, the melting parameters of DNA isolated from a healthy liver had the following values: $T_m = 71.41^\circ\text{C}$, $\Delta T = 6.63^\circ\text{C}$. Compared to the norm for tumor DNA, a decrease in T_m and an increase in ΔT are found (see Table, row noted 0, the melting without Mn^{2+} ions). An increase of the ΔT up to a value of 8.85°C and 8.23°C were observed respectively in melting curves of DNA from tumor-bearing mice liver and cancer cells. This fact indicates the destabilization of the tumor-bearing mice liver and cancer DNA due to defects in the primary and secondary structure [20]. As noted in [21, 22], an increase in the content of 5-methylcytosine leads to DNA mutations (replacement of GC pairs by AT). Defects in the secondary structure (the formation of open areas or regions of DNA with tightly bound proteins) increase the heterogeneity of tumor DNA.

The melting temperature (T_m) and melting interval (ΔT) of DNA from a healthy mice liver and tumor tissues of an untreated and treated with AgTOEPyP4 porphyrin tumor-bearing mice under different concentrations of Mn^{2+} ions

Source of DNA	[Mn^{2+}] / [DNA], M/bp	T_m , $^\circ\text{C}$	ΔT , $^\circ\text{C}$
Healthy	0	71.41±0.10	6.63±0.10
	1	75.32±0.15	3.35±0.15
	2	74.73±0.15	2.19±0.15
	3	72.65±0.10	1.90±0.10
	4	73.43±0.15	1.71±0.10
Cancer	0	69.34±0.10	8.23±0.10
	1	70.02±0.10	7.15±0.15
	2	73.38±0.15	6.90±0.20
	3	75.42±0.15	6.44±0.15
	4	75.99±0.10	5.97±0.10
Liver cancer	0	69.51±0.10	8.85±0.05
	1	73.30±0.15	8.12±0.15
	2	74.63±0.10	7.21±0.10
	3	74.25±0.15	6.85±0.15
	4	73.76±0.15	5.94±0.10
Cancer + AgTOEPyP4	0	70.88±0.10	6.70±0.10
	1	77.86±0.15	4.60±0.15
	2	76.81±0.10	2.04±0.15
	3	75.43±0.15	2.00±0.10
	4	74.74±0.10	1.79±0.15
Liver, cancer + AgTOEPyP4	0	71.08±0.05	7.06±0.05
	1	75.75±0.10	5.01±0.15
	2	73.96±0.15	2.50 ±0.15
	3	72.01±0.10	1.98±0.10
	4	72.00±0.15	1.95±0.15

A study of DNA melting in the presence of Mn^{2+} ions at different stoichiometric concentrations allows one to assess structural changes in the DNA molecules. The Mn^{2+} ions interact differently with normal and tumor DNA due to the presence of defects in the structure of tumor DNA. The essence of the method is as follows. Transition metal ions such as Mn^{2+} , due to their incomplete 3d electron

configuration, can form coordination bonds with donor atoms. Crystallographic data obtained for Mn^{2+} ions revealed chelate binding of ions with the oxygen of phosphate groups, with N(7) of guanine and O(2) of cytosine [10].

More information about defects in DNA structure can be obtained from changes in the ΔT parameter, rather than the T_m parameter. At a molar ratio of $[Mn^{2+}]/[DNA]=1$, metal ions shield the negatively charged phosphate groups of nucleic acids, which leads to an increase in the T_m value in all investigated groups (see Table).

In DNA samples of healthy animals, the Mn^{2+} ion binds to the sites of excess charge density at the guanine bases, leading to selective destabilization of GC base pairs [10, 23]. This leads to an approximation of the thermal stability of GC pairs to AT pairs and, consequently, to a narrowing of the melting interval ΔT . However, the melting range narrows sharply at a molar ratio of $[Mn^{2+}]/[DNA]=1$, and the narrowing slows at higher concentrations of Mn^{2+} ions. If there are defects in the secondary structure of tumor DNA, the access of metal ions to the defective sites is complicated, which leads to a smaller narrowing of the melting interval of tumor DNA compared to healthy. The melting parameters of the DNA isolated from the treated AgTOEPyP4 mice liver and tumor tissues were approaching the norm.

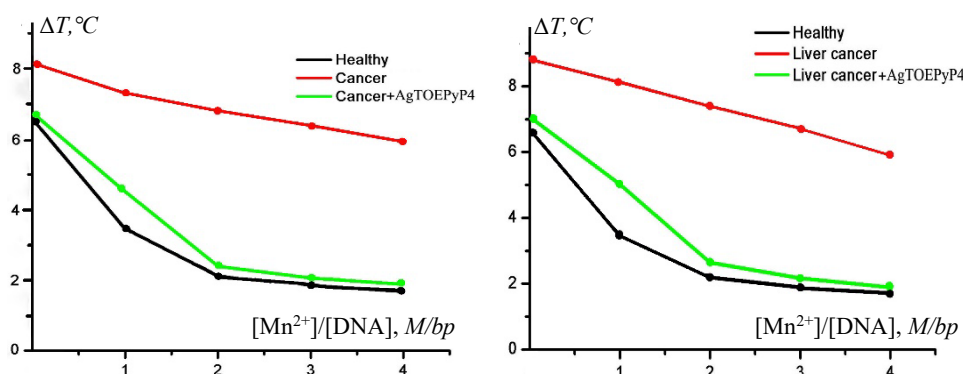


Fig. 3. The dependence of the melting interval on the $[Mn^{2+}]/[DNA]$ molar ratio in DNA samples isolated from the healthy mice liver and tumor tissues of untreated and treated with AgTOEPyP4 porphyrin mice.

Fig. 3 shows the dependencies of the melting interval ΔT on the $[Mn^{2+}]/[DNA]$ molar ratio. Upon melting of DNA isolated from healthy liver cells, the ΔT parameter was $6.63^{\circ}C$. In the presence of Mn^{2+} ions, when $[Mn^{2+}]/[DNA]=4$, a decrease in the ΔT value to $1.71^{\circ}C$ was observed. So, in healthy DNA, the ΔT parameter decreases by 3.87 ($6.63/1.71$) times at the $[Mn^{2+}]/[DNA]$ molar ratio equal to four. The same parameters calculated for DNA isolated from cancer-induced mice liver and tumor tissue were 1.48 ($8.85/5.94$) and 1.37 ($8.23/5.97$) times, respectively. According to the literature [24], this indicates the presence of defects in the structure of tumor DNA, as a result of which metal access to these sites is complicated.

The treatment of cancer-induced animals with AgTOEPyP4 porphyrin improved the liver and tumor DNA melting characteristics. As can be seen from the obtained data, the value of ΔT decreased by 3.6 ($7.06/1.95$) and 3.7 ($6.7/1.79$) times

respectively. These results revealed that the AgTOEPyP4 porphyrin closely approximates the melting parameters of the tumor DNA to the norm.

Microcalorimetry. A significant change in the calorimetric melting curve profile and shift of the curve to a lower temperature range is observed for cancer-induced mice DNA (II group) in comparison with the control (Fig. 4). The value of helix-coil transition enthalpy for healthy mice DNA was equal to 9.25 ± 0.15 kcal/mol. The melting enthalpies calculated for liver and tumor tissue of cancer-induced mice DNA were decreased to 7.24 ± 0.2 kcal/mol and 5.64 ± 0.15 kcal/mol, respectively. It should be noted that the values of transition enthalpy, for the AgTOEPyP4 porphyrin treated mice liver and tumor DNA increased to 9.1 ± 0.1 kcal/mol and 7.24 ± 0.15 kcal/mol, respectively.

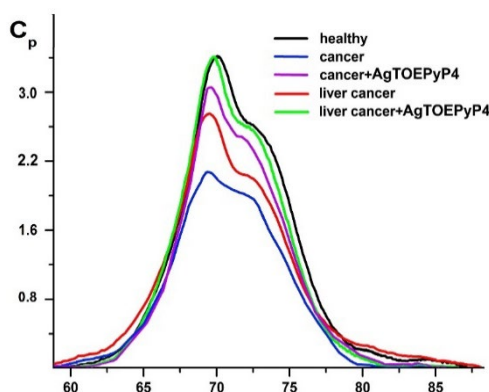


Fig. 4. Calorimetric melting curves of investigated DNA.

DNA Electrophoresis. Fig. 5 depicts the respective agarose gel electrophoresis patterns of DNA isolated from I, II and III groups.

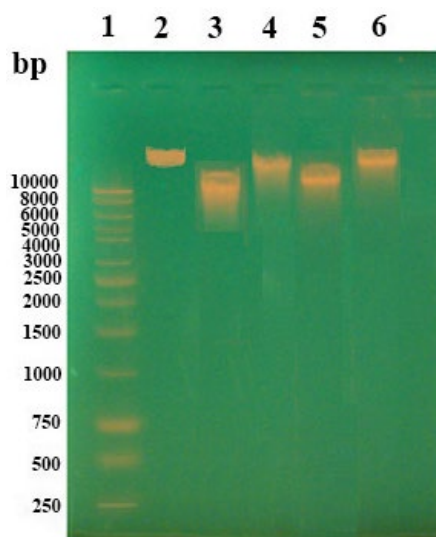


Fig. 5. DNA electrophoresis:
1) marker DNA;
2) healthy, normal DNA;
3) cancer;
4) cancer treated by AgTOEPyP4;
5) liver cancer;
6) liver cancer treated by AgTOEPyP4.

Track 1 corresponds to marker DNA. Track 2 corresponds to the normal DNA with a size of 15 kbp. The fractions corresponding to liver DNA and tumor DNA,

from cancer-induced mice are more mobile compared to healthy. The DNA fragments with different lengths are visualized in the tumor fractions. Thus, the fragments with sizes about 8–12 *kbp* and 10–13 *kbp* were found for group II mice tumor (track 3) and liver (track 5) tissues correspondingly. The DNA samples from treated by AgTOEPyP4 porphyrin mice tumor and liver have electrophoretic bands similar to healthy DNA. According to electrophoresis data, after treatment of mice, DNA fractions corresponding to sizes of 13 *kbp* and 14 *kbp* were obtained from the tumor (track 4) and liver (track 6) tissues.

Discussion. The anticancer effect of AgTOEPyP4 was investigated against mice Sarcoma S180 *in vivo*. Sarcoma 180 is an animal model of tumor, which universally used for the evaluation of anticancer drugs *in vivo* [25]. Therefore, identifying new molecules to treat these tumors is essential for improving the therapeutic and prognosis. According to the results obtained, a decrease in the tumor by up to 57% was observed in the two weeks after injections in the group of mice treated with AgTOEPyP4 porphyrin. DNA was isolated from the liver of healthy animals, from the tumor and liver of sarcoma inoculated mice untreated and treated with AgTOEPyP4 porphyrin. Structural changes in DNA were studied by melting, calorimetry, and electrophoresis methods.

We developed a novel method for detecting DNA defects during tumor formation and for evaluating the effectiveness of anticancer therapy. The thermal melting of DNA was conducted at different concentrations of Mn^{2+} ions. This makes it possible to detect DNA changes in a more pronounced form, because a significant change in the shape of the melting curves occurs depending on the concentration of Mn^{2+} metal ions. The measurement results showed that the melting parameters of DNA isolated from tumor-induced mice differ from the corresponding parameters of healthy animals. Tumor DNA contains defective regions with a disturbed primary and secondary structure. Defects in the tumor DNA structure affect the DNA melting parameters. The decrease in melting temperature testifies to DNA destabilization, which could occur due to base modifications, strand breaks or breaks of hydrogen bonds between the DNA strands. An increase in the value of T_m indicates the stabilization of the DNA molecule, possibly due to crosslink's, by the action of various ligands. Changing the ΔT parameter suggests the changing degree of DNA heterogeneity. With an increasing the defects of DNA the heterogeneity and, consequently, the ΔT parameter also increase.

The differential melting curves of tumor DNA are shifted relative to healthy DNA towards low temperatures, i.e., in tumor DNA a decrease in the melting point T_m and an increase in the melting range ΔT was observed. It was shown that the DNA melting characteristics of DNA from mice treated with AgTOEPyP4 porphyrin improved. This is especially more pronounced in the changes in the ΔT parameter (graph of the dependence of ΔT on the $[Mn^{2+}]/[DNA]$ molar ratio) (Fig. 3).

Differential scanning calorimetry monitors heat effects associated with DNA phase transitions as a function of temperature. As a result of these experiments, it was shown that the melting enthalpy of DNA isolated from the liver and tumors of cancer-induced mice decreased compared to the norm. This fact indicates the presence of damage in the DNA structure. At the same time, as a result of the

treatment of mice with porphyrin, an improvement in the values of the melting enthalpy was observed (Fig. 4).

Electrophoresis was used to identify and visualize DNA fragments. In DNA fractions isolated from the liver and tumor of mice induced by cancer, DNA fragments were found that, during electrophoresis, moved faster than normal. DNA fractions from porphyrin-treated mice have electrophoretic characteristics close to normal. Thus, porphyrins are effective pharmaceutical agents in cancer therapy.

It is known that the binding mode of porphyrins to DNA depends on the chemical features of porphyrin, the nature of the central metal, the coordination number of transition metal atoms and the peripheral substituent of the pyridylic ring as well as the conformation of DNA. The three types of binding modes such as intercalation, outside self-stacking, and outside random binding for the porphyrin-DNA complexes have been generally accepted [26]. The coordination number for Ag is four. In AgTOEPyP4 the silver ion is located in the plane of the porphyrin ring, does not form any axial ligand, and so porphyrins molecules are planar. Such metalloporphyrins easily intercalate between base pairs of DNA and at GC-rich sequences in general. AgTOEPyP4 porphyrin, being a flat molecule, intercalates in the major groove of DNA and shows selectivity for GC sequences [27]. So the effectiveness of AgTOEPyP4 porphyrin as an antitumor agent is mainly determined by the planarity and presence of a silver ion in the center of the porphyrin molecule. As a result, tumor DNA with structural defects will not fully participate in reduplication and transcription. At the same time, cationic porphyrins produce singlet oxygen, thereby causing DNA damage [28]. This will reduce the size of the tumor and restore DNA characteristics.

Conclusion. The obtained results revealed that AgTOEPyP4 porphyrin has an antitumor effect against sarcoma S180. The melting, calorimetric and electrophoretic parameters of tumor and liver DNA treated with Ag-*meso*-tetra(4-N-hydroxyethylpyridyl)porphyrin mice approach to values of healthy animals DNA. A decrease in tumor sizes by about 57% was observed in our experiments.

Statement of Human and Animal Rights Experiments were fulfilled according to the "International Recommendations on carrying out of biomedical Researches with use of Animals" (CIOMS, 1985), to the "Human Rights and Biomedicine, Oviedo Convention" (CE, 1997), to the European Convention for the Protection of Vertebral Animals Used for Experimental and Other Scientific Purposes (CE, 2005) and approved by the National Center of Bioethics (Armenia).

The authors thank Dr. Kazarian R., Dr. Tovmasyan A. and Dr. Arsenyan F. for their assistance in the work.

This work was supported by the Science Committee of the MESCS RA, in the frames of the research project No. 21T-1F244.

Received 02.02.2023

Reviewed 20.03.2023

Accepted 30.03.2023

REFERENCES

1. Kessel D., Luo Y. Intracellular Sites of Photodamage as a Factor in Apoptotic Cell Death. *J. Porphy. Phthalocyanines* **5** (2001), 181–184.
<https://doi.org/10.1002/jpp.331>
2. Oleinick N.L., Evans H.E. The Photobiology of Photodynamic Therapy: Cellular Targets and Mechanisms. *Radiation Res.* **150** (1998), 146–156.
<https://pubmed.ncbi.nlm.nih.gov/9806617>
3. Lesage S.X.H., Durham L. The Occurrence and Roles of Porphyrins in the Environment: Possible Implications for Bioremediation. *Hydrol. Sci. J.* **38** (1993), 343–354.
<https://doi.org/10.1080/02626669309492679>
4. Dougherty T.J., Gomer C.J., et al. Photodynamic therapy. *J. Natl. Cancer Inst.* **90** (1998), 889–905.
<https://doi.org/10.1093/jnci/90.12.889>
5. Lavi A., Weitman H., et al. The Depth of Porphyrin in a Membrane and the Membrane's Physical Properties Affect the Photosensitizing Efficiency. *Biophysical J.* **82** (2002), 2101–2110.
[https://doi.org/10.1016/S0006-3495\(02\)75557-4](https://doi.org/10.1016/S0006-3495(02)75557-4)
6. Che C.-M., Sun R.W.-Y., et al. Gold (III) Porphyrins as a New Class of Anticancer Drugs: Cytotoxicity, DNA Binding and Induction of Apoptosis in Human Cervix Epitheloid Cancer Cells. *Chem. Commun.* **14** (2003), 1718–1719.
<https://doi.org/10.1039/B303294A>
7. Nishida K., Tojo T., et al. Evaluation of the Correlation Between Porphyrin Accumulation in Cancer Cells and Functional Positions for Application as a Drug Carrier. *Sci. Rep.* **11** (2021), 1–10.
<https://doi.org/10.1038/s41598-021-81725-3>
8. Marzilli L. G. Medical Aspects of DNA–Porphyrin Interactions. *New J. Chem.* **14** (1990), 409–420.
9. Haroutiunian S.G., Dalian Y.B., et al. A Method for Determining the Relative Effect of Ligands on AT- and GC-Base Pairs in DNA: Applications to Metal Ions, Protons and Two Amino Acids. *Nucl. Acids Res.* **18** (1990), 6413–6417.
<https://doi.org/10.1093/nar/18.21.6413>
10. Sigel H. *Metal Ions in Biological Systems*. New York (1996).
11. Tovmasyan A., Babayan N., et al. Novel Amphiphilic Cationic Porphyrin and Its Ag(II) Complex as Potential Anticancer Agents. *J. Inorg. Biochem.* **140** (2014), 94–103.
<https://doi.org/10.1016/j.jinorgbio.2014.06.013>
12. Karapetyan N.H., Malakyan M.H., et al. Influence of Amino Acids Schiff Bases on Irradiated DNA Stability *In Vivo*. *Cell Biochem. Biophys.* **67** (2013), 1137–1145.
<https://doi.org/10.1007/s12013-013-9617-5>
13. Sambrook J., Fritsch E.F., Maniatis T. *Molecular Cloning: A Laboratory Manual* (4th ed.). NY, Cold Spring Harbor Lab. Press (2012), 91–930.
14. Wells R.D., Larson J.E., et al. Physicochemical Studies on Polydeoxyribonucleotides Containing Defined Repeating Nucleotide Sequences. *J. Mol. Biol.* **54** (1970), 465–497.
[https://doi.org/10.1016/0022-2836\(70\)90121-X](https://doi.org/10.1016/0022-2836(70)90121-X)
15. Wartell R.M., Benight A.S. Thermal denaturation of DNA molecules: a comparison of theory with experiment. *Physics Report*, **126** (1985), 67–107.
[https://doi.org/10.1016/0370-1573\(85\)90060-2](https://doi.org/10.1016/0370-1573(85)90060-2)
16. Monaselidze J., Abuladze M., et al. Characterization of Chromium-Induced Apoptosis Incultured Mammalian Cells: a Differential Scanning Calorimetry Study. *Thermochim. Acta* **441** (2006), 8–15.
<https://doi.org/10.1016/j.tca.2005.11.025>
17. Sambrook J., Russell D.W. *Agarose Gel Electrophoresis Molecular Cloning: A Laboratory Manual* (3rd ed.). Chapter 5. New York, Cold Spring Harbor (2001), 5.1–5.86.
18. Ghahramani S. *Fundamentals of Probability* (2nd ed.). New Jersey, Prentice Hall (2000), 438.
19. Hather G., Liu R. et al. Growth Rate Analysis and Efficient Experimental Design for Tumor Xenograft Studies. *Cancer Inform.* **13** (2014), 65–72.
<https://doi.org/10.1080/07391102.2021.1942216>
20. Messori L., Casini A., et al. Effects of Two Representative Antitumor Ruthenium (III) Complexes on Thermal Denaturation Profiles of DNA. *Inorganica Chim. Acta* **303** (2000), 282–285.
<http://dx.doi.org/10.1093/nar/18.21.6413>

21. Kulis M., Esteller M. 2-DNA Methylation and Cancer. *Adv. Genet.* **70** (2010), 27–56.
<https://doi.org/10.1016/B978-0-12-380866-0.60002-2>
22. Estéicio M.R.H., Issa J.P.J. Dissecting DNA Hypermethylation in Cancer. *FEBS Lett.* **585** (2011), 2078–2086.
<https://doi.org/10.1016/j.febslet.2010.12.001>
23. Saenger W. *Principles of Nucleic Acids Structure*. New-York, Springer-Verlag (1984).
24. Shin Y.A. Interaction of Metal Ions with Polynucleotides and Related Compounds. XXII. Effect of Divalent Metal Ions on the Conformational Changes of Polyribonucleotides. *Biopolymers* **12** (1973), 2459–2475.
<https://doi.org/10.1002/bip.1973.360121103>
25. Demicco E.G., Ding L., et al. Comprehensive and Integrated Genomic Characterization of Adult Soft Tissue Sarcomas. *Cell* **171** (2017), 950–965.
<https://doi.org/10.1016%2Fj.cell.2017.10.014>
26. Pasternack R.F. Circular Dichroism and the Interactions of Water Soluble Porphyrins with DNA. A Minireview. *Chirality* **15** (2003), 329–332.
<https://doi.org/10.1002/chir.10206>
27. Ananyan G.V., Karapetyan N.H., Dalyan Y.B. The Structural Features of Poly(dG-dC).poly(dG-dC) at Complexation with Some Porphyrins. *J. Biomol. Struct. Dyn.* **40** (2022).
<https://doi.org/10.1080/07391102.2021.1942216>
28. Fiel R.J. Porphyrin-Nucleic Acid Interactions: A Review. *J. Biomol. Struct. Dyn.* **6** (1989), 1259–1275.
<https://doi.org/10.1080/07391102.1989.10506549>

Ն. Հ. ԿԱՐԱՊԵՏՅԱՆ, Գ. Վ. ԱՆԱՆՅԱՆ, Ս. Գ. ՀԱՐՈՒԹՅՈՒՆՅԱՆ

AgTOEPyP4 ՊՈՐՓԻՐԻՆԻ ՀԱԿԱՌԻՌՈՒՑՔԱՅԻՆ ԱԶԴԵՑՈՒԹՅՈՒՆԸ

Արձաթ պարունակող պորֆիրինը Ag-meso-tetra(4-N-hydroxyethylpyridyl)porphyrin (AgTOEPyP4) հետազոտվել է որպես պոտենցիալ հակաուռուցքային դեղամիջոց՝ օգտագործելով սպեկտրոֆոտոմետրիկ, կալորիմետրիկ և էլեկտրաֆորետիկ չափումներ: Ուսումնասիրություններն իրականացվել են առողջ, քաղցկեղով հիվանդ և AgTOEPyP4-ով բուժված սպիտակ մկների վրա: ԴՆԹ-ն անջատվել է մկների յարդից և ուռուցքային հյուսվածքներից: Հալման կորերը ուսումնասիրվել են Mn^{2+} իոնների տարբեր ստեխիոմետրիկ կոնցենտրացիաների առկայությամբ: Հալման բնութագրերի միջոցով պարզվել է, որ ուռուցքից անջատված ԴՆԹ-ի հետ Mn^{2+} իոնների փոխազդեցության բնույթը տարբերվում է նորմալից՝ ի հաշիվ երկրորդային կառուցվածքում առկա դեֆեկտների: Պարզվել է, որ ուռուցքակիր մկների հյուսվածքներից անջատված ԴՆԹ-ի հալման պարամետրերը, էնթալպիան և էլեկտրաֆորետիկ շարժունակությունը տարբերվում են առողջ հյուսվածքների ԴՆԹ-ի համապատասխան պարամետրերից: Ցույց է տրվել, որ AgTOEPyP4-ով բուժված մկների յարդից և ուռուցքից անջատված ԴՆԹ-ի հետազոտված բոլոր պարամետրերը մոտեցել են նորմալին: Ստացված արդյունքները թույլ են տալիս եզրակացնել, որ AgTOEPyP4 պորֆիրինն ունի ընդգծված թերապևտիկ ազդեցություն S180 սարկոմայի դեմ և պահանջում է հետագա հետազոտություն՝ որպես հակաքաղցկեղային դեղամիջոց:

Н. Г. КАРАПЕТЯН, Г. В. АНАНЯН, С. Г. АРУТЮНЯН

ПРОТИВОПУХОЛЕВЫЙ ЭФФЕКТ ПОРФИРИНА AgТОЕРуР4

Серебросодержащий порфирин Ag-мезо-тетра(4-N-гидроксиэтилпиридил)порфирин (AgТОЕРуР4) был исследован как потенциальное противоопухолевое средство с помощью спектрофотометрических, калориметрических и электрофоретических измерений. Исследования проводились на здоровых, индуцированных раком и пролеченных порфирином AgТОЕРуР4 белых мышах. ДНК выделяли из печени и опухолевых тканей мышей. Кривые плавления изучали в присутствии различных стехиометрических концентраций ионов Mn^{2+} . Характер взаимодействия ДНК– Mn^{2+} в опухоли отличается от такового в норме из-за дефектов вторичной структуры, что выражается в характеристиках плавления ДНК. Выявлено, что параметры плавления, энтальпия и электрофоретическая подвижность ДНК, выделенной из тканей мышей-опухоленосителей, отличались от таковых для ДНК здоровых мышей. Показано, что все изученные параметры ДНК, выделенной из печени и опухоли мышей, обработанных AgТОЕРуР4, приближаются к норме. Полученные результаты позволяют предположить, что порфирин AgТОЕРуР4 обладает выраженным терапевтическим действием в отношении саркомы S180 и требует дальнейшего изучения в качестве противоопухолевого препарата.